ANL-6595

Argonne National Laboratory

A SUBCRITICAL PLUTONIUM-FUELED FAST REACTOR CORE (ZPR-III Assembly 37)

by

P. I. Amundson, R. Jiacoletti,
J. K. Long, and R. L. McVean

ANL-6595
Reactor Technology
(TID-4500, 17th Ed.)
AEC Research and
Development Report

ARGONNE NATIONAL LABORATORY
9700 South Cass Avenue
Argonne, Illinois

A SUBCRITICAL PLUTONIUM-FUELED FAST REACTOR CORE (ZPR-III Assembly 37)

by

P. I. Amundson, R. Jiacoletti,*
J. K. Long, and R. L. McVean

Idaho Division

*Resident Research Associate from University of Wyoming presently at Argonne National Laboratory, Idaho Division.

July 1962

Operated by The University of Chicago
under
Contract W-31-109-eng-38

TABLE OF CONTENTS

LIST OF FIGURES

LIST OF FIGURES

LIST OF TABLES

A SUBCRITICAL PLUTONIUM-FUELED FAST REACTOR CORE (ZPR-III* Assembly 37)

by

P. I. Amundson, R. Jiacoletti,
J. K. Long, and R. L. McVean

ABSTRACT

A subcritical fast reactor, fueled with plutonium, is described. Calculations and experimental measurements of neutron flux and gamma dose rates near the bare core face are reported, as well as the core temperature increase due to plutonium alpha and gamma heating.

I. INTRODUCTION

ZPR-III Assembly 37, a subcritical plutonium-fueled fast reactor, was constructed to measure several parameters of the core that would materially help in writing a hazards analysis for future plutonium critical loadings in ZPR-III. The assembly design was based on the fuel and diluent ratios of Assembly 2(9) and is anticipated to be similar to one of the initial critical plutonium assemblies that will be run in the future.

Neutron flux and gamma dose rates were measured near the face of this assembly. Temperature measurements were made periodically at 36 points within the assembly, so that both axial and radial temperature distributions as well as temperature rise in the core due to alpha heating from the plutonium fuel could be determined. The maximum temperature rise in the core was determined by insulating the front face of the assembly with 3 in. of Fiberglas insulation and measuring the core saturation temperatures.

Approximate calculations were made for gamma dose rate and neutron flux between the assembly halves and compared with experimental results.

---

*A detailed description of ZPR-III can be found in Ref. 1.

A SUBCRITICAL PLUTONIUM-FUELED FAST REACTOR CORE (ZPR-III* Assembly 37)

by

P. I. Amundson, R. Jacoviatti,
J. K. Long, and R. L. McVean

ABSTRACT

A subcritical fast reactor, fueled with plutonium, is described. Calculations and experimental measurements of neutron flux and gamma dose rates near the bare core face are reported, as well as the core temperature increase due to plutonium alpha and gamma heating.

I. INTRODUCTION

ZPR-III Assembly 37, a subcritical plutonium-fueled fast reactor, was constructed to measure several parameters of the core that would materially help in writing a hazards analysis for future plutonium critical loadings in ZPR-III. The assembly design was based on the fuel and diluent ratios of Assembly 36 and is anticipated to be similar to one of the initial critical plutonium assemblies that will be run in the future.

Neutron flux and gamma dose rates were measured near the face of this assembly. Temperature measurements were made periodically at 36 points within the assembly, so that both axial and radial temperature distributions as well as temperature rise in the core due to alpha heating from the plutonium fuel could be determined. The maximum temperature rise in the core was determined by insulating the front face of the assembly with 3 in. of Fiberglas insulation and measuring the core saturation temperatures.

Approximate calculations were made for gamma dose rate and neutron flux between the assembly halves and compared with experimental results.

---

*A detailed description of ZPR-III can be found in Ref. 1.

II. DESCRIPTION OF ASSEMBLY 37

Assembly 37 was constructed entirely in one half of the bisectional ZPR-III reactor. This assembly duplicates approximately half of a critical system, and allows easy extrapolation of measurements to the full assembly with each half containing an equal part of the critical mass. The cylindrical core was partially blanketed with full-density depleted uranium. Several physical parameters of this core are given in Table I.

Table I

PHYSICAL PARAMETERS OF CORE

Mass of Plutonium (kg)		20.05
Plutonium Analysis (%)	Pu^{239}	95
	Pu^{240}	4.5
	Pu^{241}	0.5
Core Length (in.)		8
(cm)		20.3
Core Radius (in.)		7.68
(cm)		19.5
Core Volume Fractions		
Plutonium		0.04
Depleted Uranium		0.15
Stainless Steel		0.12
Aluminum		0.31

The material densities in gm/cm^3 used to calculate the core volume fractions were as follows: plutonium, 19.06; depleted uranium, 19; stainless steel, 7.85, and aluminum, 2.7.

Each core drawer contained two $\frac{1}{8}$-in. columns of plutonium, 3 columns of depleted uranium, and 11 columns of aluminum. The 11 columns of aluminum were divided into 6 columns of 63%-aluminum and 5 columns of 45%-aluminum. The material arrangement for the standard core drawer is shown in Fig. 1. A face view of the assembly is shown in Fig. 2.

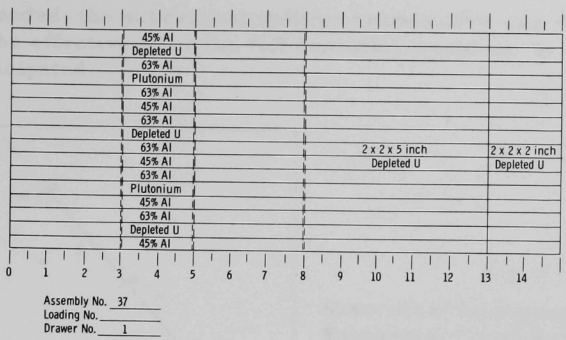

Fig. 1. Typical Arrangement of Materials in Core Drawer

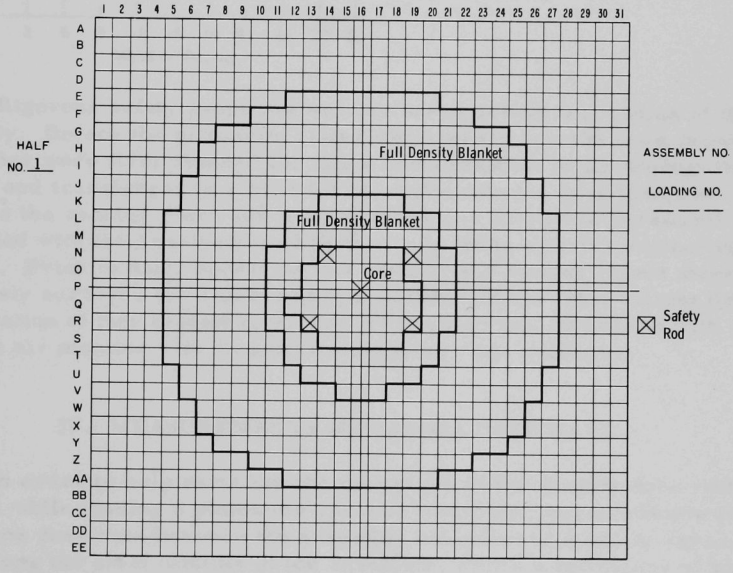

Fig. 2. Face View of Assembly 37

III. LOADING OF ASSEMBLY

Although the effective k of this assembly was expected to be between 0.3 and 0.5, it was loaded in a manner similar to the procedure usually followed in constructing a critical assembly. A plot of inverse count rate vs. mass of plutonium in the assembly at the time is given in Fig. 3. As

loading proceeded, the subcritical multiplication curve was checked to insure that the effective k for the full assembly would not be far greater than that anticipated.

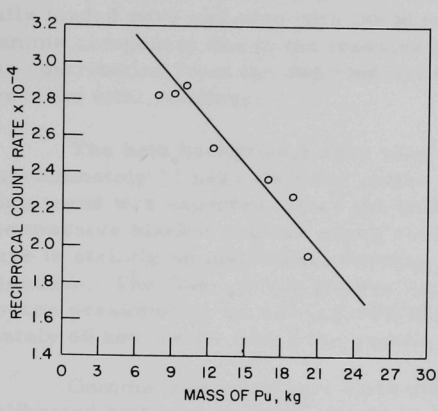

Fig. 3

Subcritical Multiplication Curves: Reciprocal Count Rate Vs. Mass of Pu

Rigorous safety practices were followed during the loading of this assembly. Before the plutonium plates were loaded into the core drawers, the former were first checked for alpha contamination in an internal flow counter and transferred to a hood for insertion into the core drawers. Entrance to the reactor room and loading room was limited to personnel associated with the assembly, and then only to those wearing protective clothing. Prior to daily operation, the reactor and loading rooms were completely surveyed for alpha-emitting contamination. At all times during the operation of this assembly the assembly room was monitored with a stepwise air monitor with an annular-impactor-type collector.

IV. MEASUREMENTS OF GAMMA DOSE RATE

In order to help establish the magnitude of the gamma dose rates expected while loading a plutonium critical assembly, measurements of the gamma dose rate between the assembly halves were made at several points along the axial midline of the assembly. Since a knowledge of gamma intensities is primarily a health problem, health-physics instruments were used to make the measurements. The gamma survey meters used were of the ion chamber variety, commonly called the Juno. These instruments have a rectangular air-ionization chamber with movable shutters on the lower face designed to permit 3 different types of measurements: alpha + beta + gamma readings, beta + gamma readings, or gamma readings alone. The instruments can be calibrated only in dose rate units for gamma radiation, but if large amounts of low-energy gamma radiation should possibly be present near this assembly, the beta-gamma and alpha-beta-gamma

readings are then an indication of the existence of this large low-energy component of gamma radiation.

Measurements were taken with the shutters in all positions with the fully loaded core and also with the plutonium removed; thus the beta-and-gamma component due to the massive blanket of depleted uranium and also the contribution from the depleted uranium in the core could be subtracted from the total readings.

The beta background dose rate, as read on the meters, rose from approximately 13 near the core center to 25 mr/hr at 29 in. from the core. This trend was expected, since the bulk of the beta radiation emanates from the massive blanket regions which surround the core. The term mr/hr here is strictly an instrument reading, not a measured dose rate for beta radiation. The Juno survey meters were calibrated with a radium gamma source presumed to be within ± 10% of this calibration down to approximately 80 kev, below which the gamma efficiency falls off rather rapidly.

Gamma measurements were also made with dental-type X-ray films, calibrated both with radium gamma radiation and a 50-kvp X-ray machine. The films were placed at various radii on the core interface and also at a distance of 29 in. from the core interface. Since the film sensitivity varies considerably between the 2 energy calibrations, and since the effective gamma energy emitted from this core is probably somewhere between these 2 energies, little can be said of the measured dose rates using these films. It is expected that the average energy of gamma rays emitted from this assembly will be in the region of 60-80 kev; therefore, one would assume that the radium gamma calibration is more realistic than the X-ray calibration.

The results of the gamma measurements are given in Table II.

Table II

MEASUREMENTS OF GAMMA DOSE RATE

Distance from Core (in.) (measured to front of detector)	Radiation Admitted into Ion Chamber	Juno Reading (mr/hr)	X-ray Film	
			Radium Calibration (mr/hr)	50 kvp Calibration (mr/hr)
0	γ	66	260	21
	$\beta\gamma$	69		
	$\alpha\beta\gamma$	71		
3	γ	42		
	$\beta\gamma$	43		
	$\alpha\beta\gamma$	44		
6	γ	32		
	$\beta\gamma$	33		
	$\alpha\beta\gamma$	34		
12	γ	16		
	$\beta\gamma$	18		
	$\alpha\beta\gamma$	21		
20	γ	9		
	$\beta\gamma$	11		
	$\alpha\beta\gamma$	12		
29	γ	6	7	0.5
	$\beta\gamma$	6		
	$\alpha\beta\gamma$	6		

If the average gamma-ray energy is in the region of 60-80 kev, as expected, the 12-20- and 29-in. Juno readings will probably be low, but should not be in error by more than 30%. Measurements taken closer in should be more in error due to the larger component of oblique radiation absorbed by the thicker side walls of the ion chamber. The surface Juno and X-ray readings are not comparable, since the X-ray films were taped directly to the core face while the Juno readings were made with the instrument touching the face, resulting in an effective ionization chamber center approximately 2 in. away from the core interface. In all cases with the Juno survey meter, the effective distance between core interface and ionization chamber center should be taken as the measured distance plus 1.5 in.

All measurements have been corrected for background radiation (mostly beta) emitted from the depleted uranium in the assembly. Background measurements were made with the entire core intact, except for the plutonium fuel.

Figure 4 shows a plot of the gamma dose rate vs. distance from the core face as measured with the Juno survey meter and also the calculated falloff of dose rate from a plane circular disk positioned at the core interface.

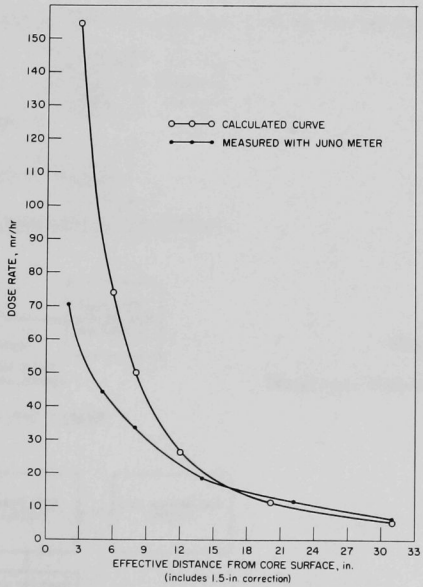

Fig. 4. Gamma Dose Rate along Axial Midline

V. NEUTRON-FLUX MEASUREMENTS

The fast neutron flux was measured with 3 different types of neutron detectors at a point midway between the 2 assembly halves (29 in. from the core interface). Measurements were made first with a lithium iodide crystal surrounded by polyethylene spheres of varying diameters. Bonner[2] indicates that an average neutron energy as well as total neutron flux can be measured with this instrument.

The second type of detector used was an RCL fast-neutron survey meter. This survey meter uses a methane-filled, polyethylene-lined proportional counter whose response is such that the number of counts produced is approximately proportional to the first collision depth dose for neutrons between 0.2 and 10 Mev.[3] Although this detector was not designed to measure neutron flux, a reasonable approximation can be made if one corrects the count rate for the rather well-known energy dependence of this counter. This correction, of course, depends on a knowledge of the average neutron energy.

The third type of detector used was a Hanson-Long Counter. This counter was designed specifically to measure neutron flux, and its efficiency is essentially constant between approximately 10 kev and several Mev.[4]

Block diagrams of these systems can be found in Fig. 5.

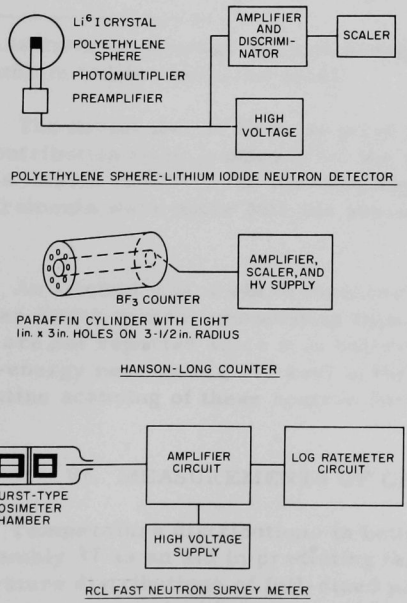

Fig. 5

Neutron-detection Systems

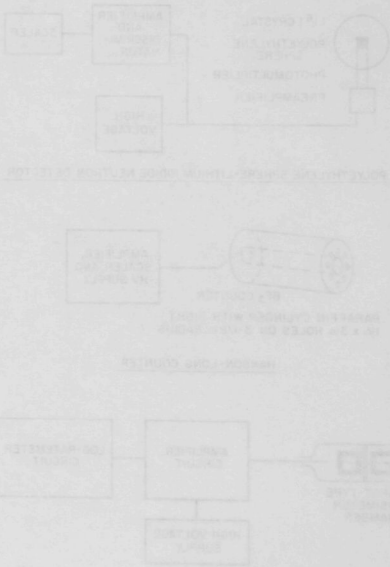

The neutron flux was also measured at a point roughtly 4 in. from the core interface on the core cylindrical axis with the RCL fast-neutron survey meter. Positioning problems and finite detector volumes limit the accuracy of this measurement by the estimate of distance from the core interface to the effective detector center. The results of these measurements corrected for background are given in Table III. The results of the lithium iodide measurements are not given because of calibration uncertainties.

Table III

NEUTRON FLUX MEASUREMENTS

Distance from Core Face	Instrument	Reading (n_f/cm^2-sec)
29 in. (midway between halves)	Modified "Hanson and Long Counter"	70
29 in.	RCL Fast Neutron Survey Meter	60*
Instrument at Contact (effective distance ≈ 4 in.)	RCL Fast Neutron Survey Meter	171

*Assuming an average neutron energy of 400 kev (estimated from lithium iodide measurements).

The actual flux at 29 in. is more nearly 90 n_f/cm^2-sec due to a 30% contribution from leakage from the startup source cask and spontaneous fission of U^{238} in the massive depleted-uranium blanket. All measurements were made with the sources in their respective source casks.

An attempt was made to measure the surface neutron flux with Eastman Kodak neutron-monitoring film. The results of these measurements are not reported since it is believed that the very large component of low-energy neutrons (< 300 kev) in the spectrum may go undetected in the routine scanning of these neutron films.

VI. MEASUREMENTS OF CORE TEMPERATURE

Temperature distributions in both space and time were measured in Assembly 37 as an aid in predicting the temperature rise and spatial temperature distributions of full-sized plutonium assemblies. Temperatures were measured with iron-constantan thermocouples placed at

36 points within the assembly. The thermocouple potentials were measured with a Leeds and Northrup type K-2 potentiometer and light beam galvanometer. A block diagram of the measuring circuit can be found in Fig. 6. The thermocouple Type IC calibration is shown in Fig. 7.

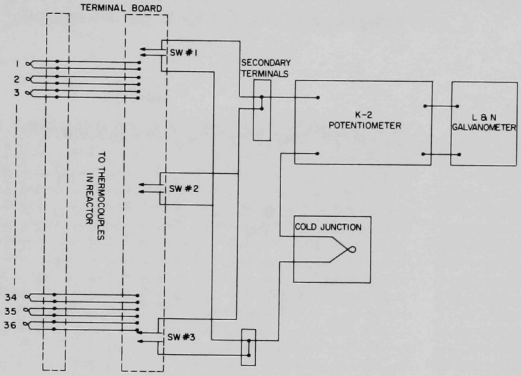

Fig. 6. Temperature-measuring Circuit

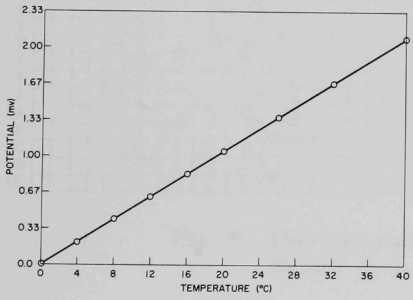

Fig. 7

Type IC Thermocouple Calibration

The thermocouples were placed in the assembly so that a 3-point axial distribution at several different radii could be generated. Thermocouples also touched different materials to obtain a qualitative, general idea of thermal contact between pieces in the assembly. Several thermocouples were placed in channels formed by the curved edge of 4 adjacent matrix tubes; others were placed touching the lower edge of depleted uranium, plutonium cans, and aluminum pieces. To obtain the maximum

core temperature, 3 thermocouples were placed touching the center of the sides of the plutonium fuel cans in a central drawer. The specific positions of thermocouples are shown in Fig. 8, 9 and 10. All 36 thermocouples were read several times each day so that the time dependence of temperature could be analyzed. After the bare-face-core saturation temperature had been reached, a 3-in.-thick blanket of Fiberglas insulation was placed over the bare core face, and temperatures were again measured vs. time until a new saturation temperature was reached. If heat loss through the Fiberglas insulation can be ignored, this saturation temperature will be the same as that temperature reached with the halves together, each containing 20 kg of plutonium in this type of configuration.

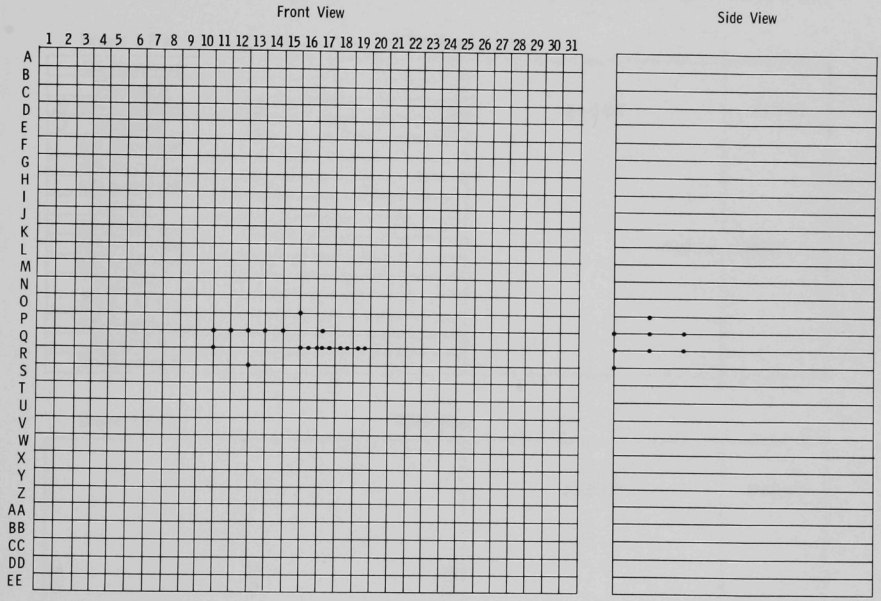

Fig. 8. Thermocouple Positions in the Core (Scale: $\frac{1}{10}$ in. = 2 in.).

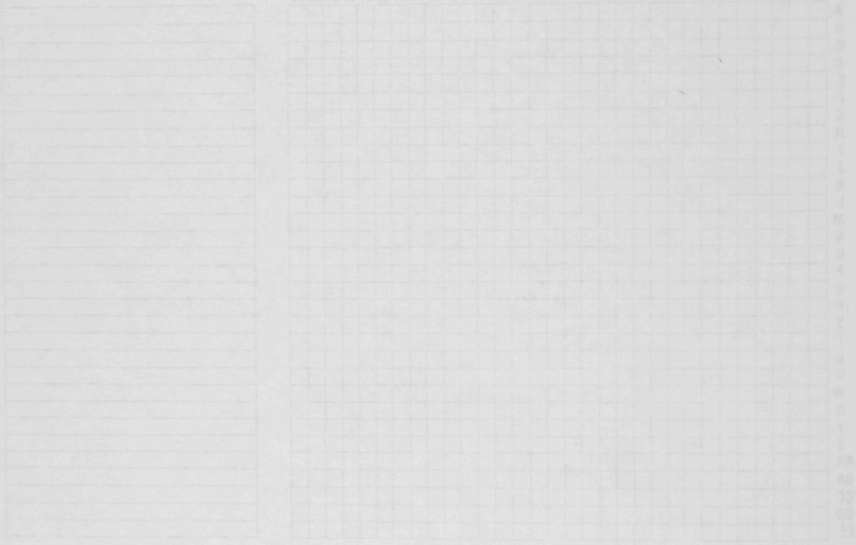

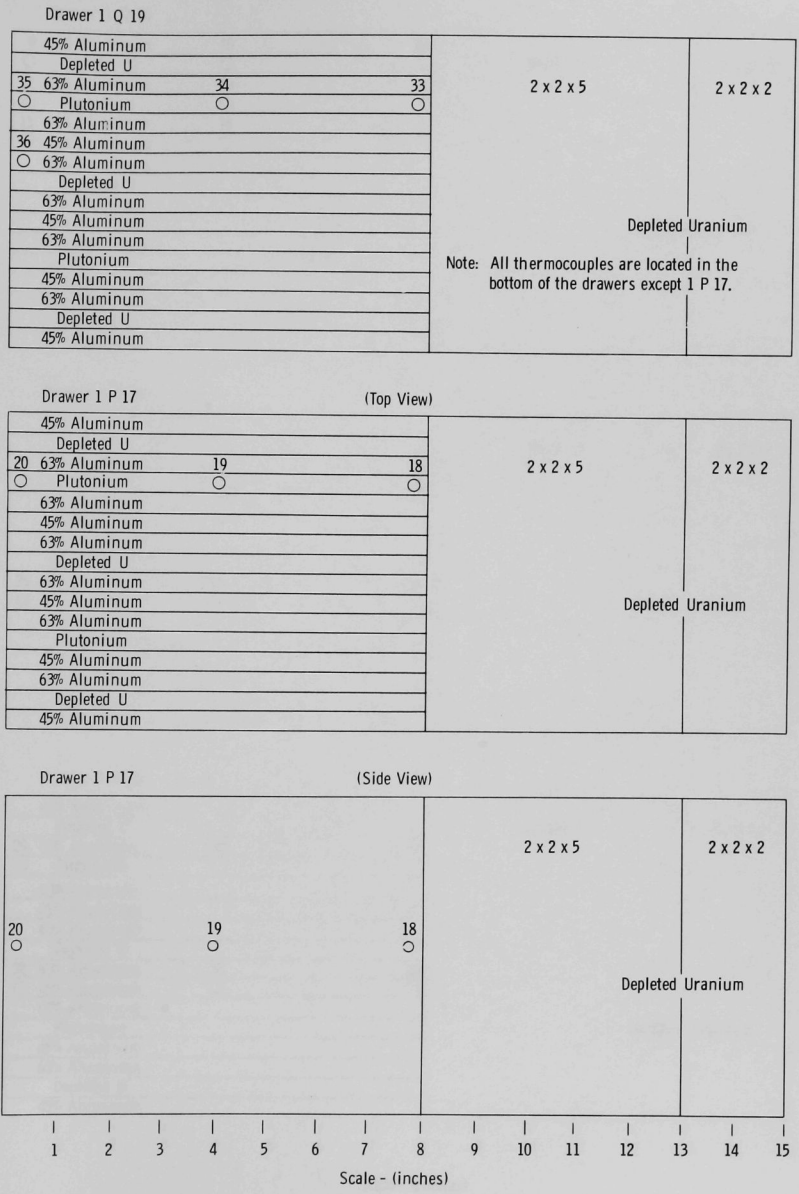

Fig. 9. Thermocouple Positions in Some Core Drawers

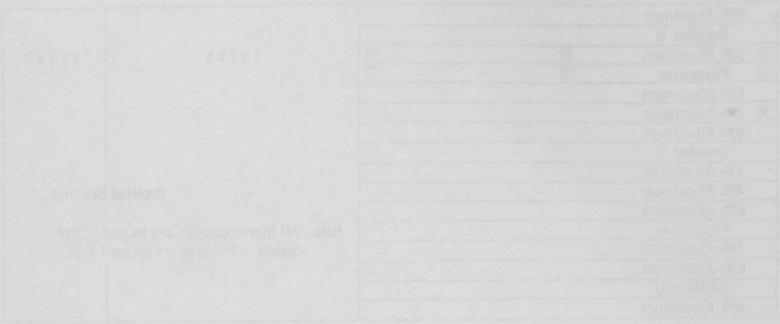

Drawer 1 Q 16

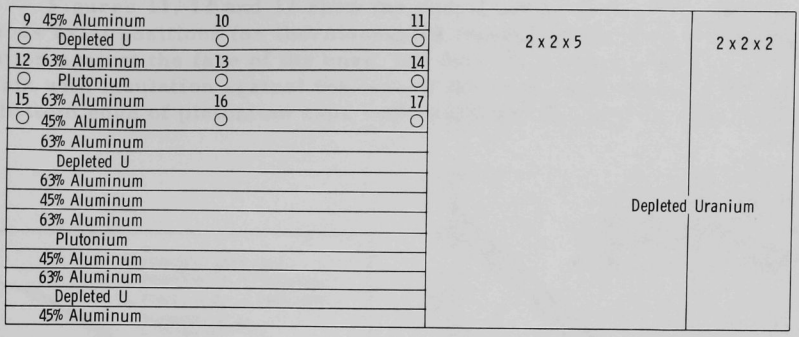

Drawer 1 Q 17

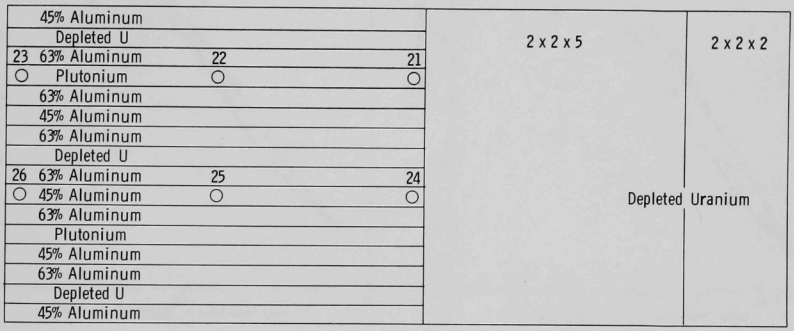

Drawer 1 Q 18

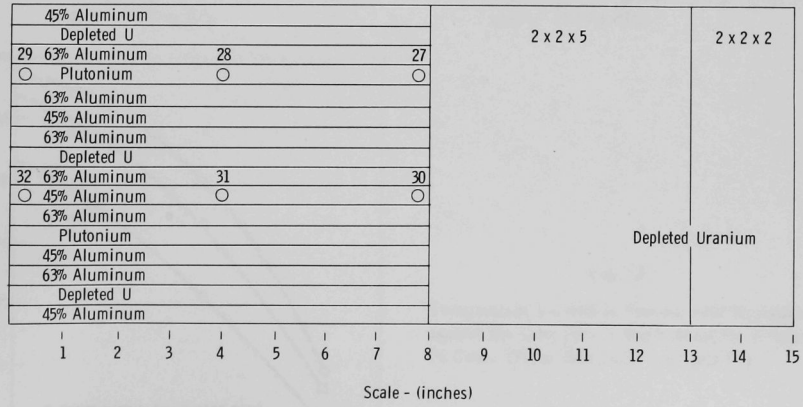

Fig. 10. Thermocouple Positions in Other Core Drawers

Figures 11, 12 and 13 show the radial temperature distributions at various axial positions for thermocouples located in the matrix with no insulation against the face of the core, for thermocouples located in the matrix with insulation against the face of the core, and for those touching the bottom edge of plutonium cans with insulation against the core face.

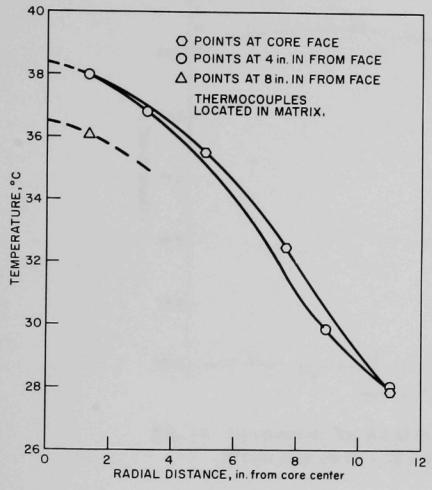

Fig. 11. Temperature Vs. Radial Position with no Insulation against Face (From data 16:00 - 12 July 61).

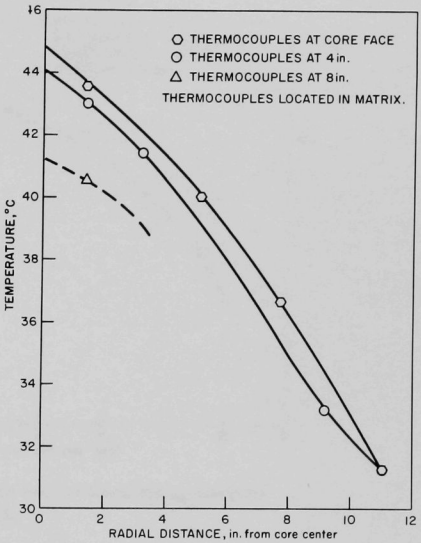

Fig. 12. Temperature Vs. Radial Position at Saturation with Insulation against Face (From data 15:45 - 17 July 61).

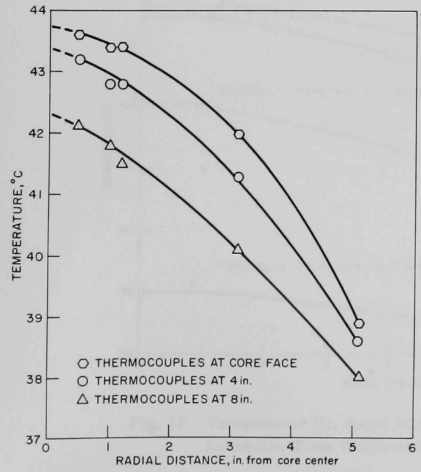

Fig. 13

Temperature Vs. Radial Position with Insulation against the Core Face - Thermocouples Touching Pu Cans. (From data 15:45 - 17 July 61).

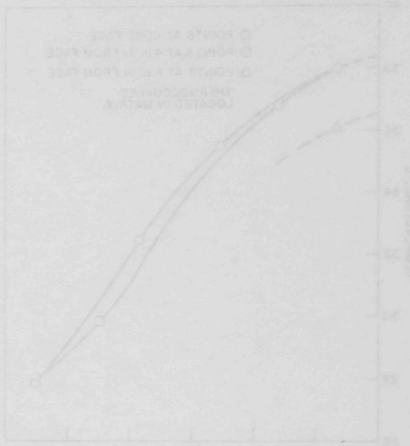

Figures 14 and 15 show the axial temperature distributions without insulation against the core face and with insulation against the core face. It will be noted that the maximum temperature occurred at a point 4 in. into the assembly with no insulation against the core face. With insulation against the core face the maximum temperature occurred at the core interface. The 8-in. point on the second curve from the top of Fig. 15 is probably high.

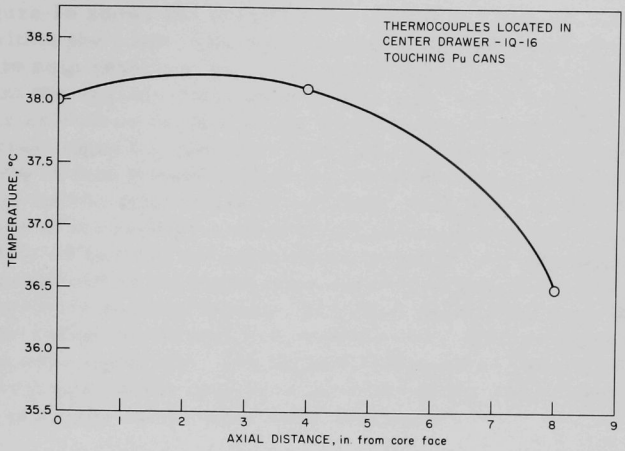

Fig. 14. Temperature Vs. Axial Position with no Insulation against Face (From data 16:00 - 12 July 61).

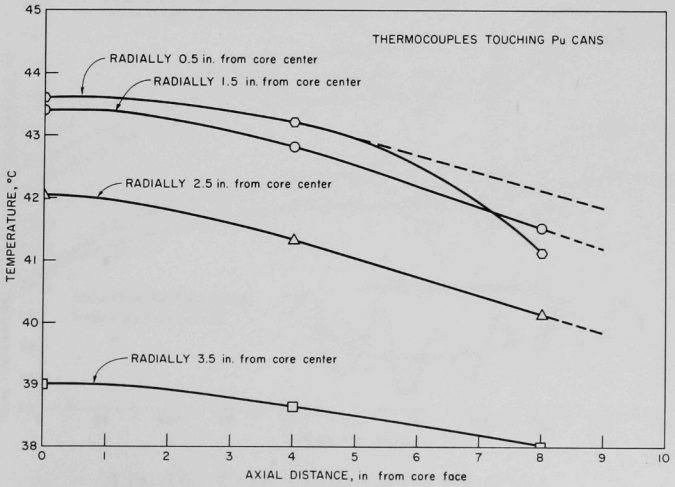

Fig. 15. Temperature Vs. Axial Position with Insulation against Face at Saturation Time (From data 15:45 - 17 July 61).

In general, temperatures of thermocouples touching both depleted uranium and aluminum pieces showed temperatures equal to those thermocouples touching plutonium fuel cans in the same area. This, in conjunction with equal temperatures of thermocouples touching plutonium pieces and thermocouples inserted in slots between matrix tubes, indicates that the general thermal contact within the core was quite good.

Figure 16 shows the temperature rise of the core vs. time for several positions within the core. The room-temperature distribution vs. time is also given to help explain some of the core-temperature deviations. It should be noted that the reactor room temperature had rather drastic daily temperature cycles as well as large average room-temperature fluctuations over a 5-day interval. Since the assembly was rather massive, it was thought that the deviations of core temperature from a smooth rise occurred because of the slow average room-temperature oscillations. It appears that if the frequency and amplitude of the average room-temperature oscillations are constant, approximately 24 hr exist between room-temperature peaks and corresponding peaks measured by thermocouples near the center of the core. The maximum temperature reached with no insulation against the core face was 39.5°C at the radial center and 4 in. into the core. This temperature occurred 128 hr after core assembly. The highest temperature (43.6°C) recorded with insulation against the core face occurred at the radial core center and at the core interface 222 hr after core assembly.

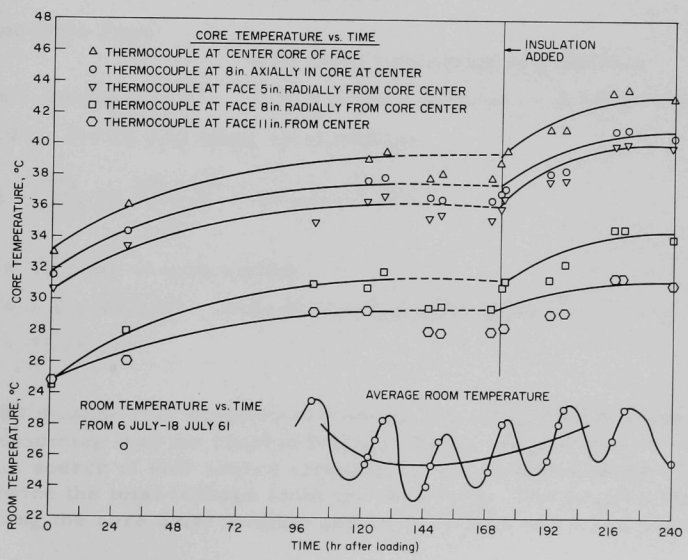

Fig. 16. Core Temperature Vs. Time

VII. ESTIMATE OF NEUTRON FLUX LEAKING FROM FRONT FACE OF ASSEMBLY

The effective k (reactivity) of this assembly was calculated by means of multigroup transport theory. The problem, run on an IBM 704 computer, used the 11-group cross-section set (Set 58)(10) and the two-dimensional transport theory code for a finite cylinder (TDC code).(11)

The solution to the problem indicated an effective k of 0.49, resulting in a multiplication of approximately 2.0. The pointwise neutron flux, total transport cross sections, and total leakage printouts were used to calculate the amount of leakage through the face of the reactor both for the core area and the blanket area at the open face. The results given in Table IV show that the bulk of the neutron leakage from this reactor comes out of the core face.

Table IV

CALCULATION OF NEUTRON FLUX BETWEEN ASSEMBLY HALVES

Source Strength =	20 kg x 6.2×10^4 n/sec-kg(Pu) = 1.24×10^6 n/sec
Calculated Leakage =	9.998×10^5 n/sec, from printout normalized to real source
Fractional Open Face Leakage =	0.96 from calculation of gradients
Front Face Leakage S_f =	0.96 x 9.998 x 10^5 n/sec = 9.598×10^5 n/sec

Flux at 29 in. (73.66 cm) along axial midline:

$$\phi = \frac{2S_f}{4(A)} \ln \frac{(r^2 + a^2)}{a^2} = 29 \text{ n/cm}^2\text{-sec}$$

where r = 19.5 cm = core radius

A = 1.1×10^3 cm^2 = area of face (circular disk)

a = 73.66 cm

The midline flux equidistant between the reactor halves was calculated by assuming that the reactor leakage can be represented by an isotropic disk source of unit source strength $S\phi$ and radius r, where $S\phi$ is equal to twice the total leakage from the core face. The neutron flux at a point along the core axial midline and 29 in. (73.66 cm) away will be

$$\phi = S\phi/4 \ln \frac{(r^2 + a^2)}{a^2}$$

VII. ESTIMATE OF NEUTRON FLUX LEAKING FROM FRONT FACE OF ASSEMBLY

The effective k (reactivity) of this assembly was calculated by means of multigroup transport theory. The problem, run on an IBM 704 computer, used the 11-group cross-section set (Set 5S)[10] and the two-dimensional transport theory code for a finite cylinder (TDC code).[11]

The solution to the problem indicated an effective k of 0.49, resulting in a multiplication of approximately 2.0. The poisonwise neutron thru total transport cross sections, and total leakage probabilities were used to calculate the amount of leakage through the face of the reactor both for the core area and the blanket area at the open face. The results given in Table IV show that the bulk of the neutron leakage from this reactor comes out of the core face.

Table IV

CALCULATION OF NEUTRON FLUX BETWEEN ASSEMBLY HALVES

Source Strength = 20 kg x 0.4 x 10^4 n/sec-kg(^{252}Cf) = 1.24×10^5 n/sec

Calculated Leakage = 9.998×10^3 n/sec, from primout normalized to real source

Fractional Open Face Leakage = 0.98 from calculation of gradients

Front Face Leakage Sf = $0.98 \times 9.998 \times 10^3$ n/sec = 9.798×10^3 n/sec

Flux at 29 in. (73.66 cm) along axial midline:

$$\phi = \frac{2Sf}{4(A)} \ln \frac{(r_c^2 + a^2)}{r_c^2} = 29 \text{ n/cm}^2\text{-sec}$$

where r = 19.5 cm = core radius

A = 1.1×10^3 cm^2 = area of face (circular disk)

a = 73.66 cm

The midline flux equivalent between the reactor halves was calculated by assuming that the reactor leakage can be represented by an isotropic disk source of unit source strength Sf and radius r, where Sf is equal to twice the total leakage from the core face. The neutron flux at a point along the core axial midline and 29 in. (73.66 cm) away will be

$$\phi = Sf/4 \ln \frac{(r_c^2 + a^2)}{r_c^2}$$

The results of this calculation (shown in Table IV) indicate a flux approximately equal to half of the flux measured experimentally at this point. The large discrepancy between the experimental measurements and the calculated flux could exist in (1) the inability of the preceding calculation to predict accurately the neutron leakage, or (2) the contribution from multiplication of startup source neutrons (sources in shielded casks) as well as environmental scattering coupled with the nondirectional characteristics of the specific counters used in measuring the centerline flux.

VIII. ESTIMATE OF GAMMA DOSE RATES

Gamma-ray dose rates at several points along the core axial midline have been approximated. Roesch[8] has calculated the surface dose rates of large pieces of pure isotopes of plutonium and their significant decay products. The surface dose rates (absorbed dose) for the important isotopes are listed in Table V for an isotope mixture initially containing 95% plutonium-239, 4.5% plutonium-240, 0.5% americium-241, and 0.5% uranium-237. The T_1 column represents the surface dose rates 4 months after the above analysis date and T_2 represents the dose rates after 2 years. The plutonium fuel surface dose rates (D_p) are represented by column T_2 at the time the experiment was conducted. Column T_1 is presented for comparison only.

Table V

SURFACE DOSE RATES FOR PLUTONIUM FUEL

Isotope	Component	Fuel Fraction	Rad/hr-unit Surface Area: Pure Isotope[8] Dose Rate	Rad/hr-unit Surface Area: T_1	Rad/hr-unit Surface Area: T_2
Pu^{239}	X-rays	0.95	0.61	0.5795	0.5795
	hard	0.95	0.056	0.0532	0.0532
Pu^{240}	X-rays	0.045	14	0.630	0.630
	hard	0.045	0.37	0.0167	0.0167
(fission product equilibrium)	hard	0.045	0.25	0.0113	0.0113
Am^{241}	X-rays	0.005	$(237 \times 4.28 \times 10^{-4}t)$*	0.072	0.432
	hard	0.005	$(221 \times 4.28 \times 10^{-4}t)$*	0.068	0.408
U^{237}	hard	0.005	$(23 \times [1-e^{-0.102t}])$*	0.115	0.115
Plutonium Fuel	X-rays			1.282	1.642
	hard			0.264	0.604
	Total			1.546	2.246

*t in days; for times much less than 14 yrs.

The above analysis was based on the high absorption properties of plutonium for the low-energy gamma rays emitted. If we are willing to assume that this homogenized core is also highly absorbing (a reasonable assumption for 20-kev X-rays), the core unit surface dose rate becomes

$$D_f = \frac{D_p A_f}{A_c} = 2.246 \times \frac{0.3039}{4.75} = 0.1436 \text{ rad/hr-cm}^2 \text{ core area} \quad ,$$

where A_f/A_c is the fractional area of the core face occupied by plutonium fuel.

Since the surface dose rate is due mostly to gamma rays emitted very near the core face, the flux distribution will be nearly that of circular disk source. Therefore, the axial midline dose rate at any distance a for a core of radius r can be represented by

$$D_a = \frac{D_c}{4} \ln \left(\frac{r^2 + a^2}{a^2} \right) \quad ,$$

where

$$D_c = 2 D_f \quad .$$

At a point midway between the ZPR-III assembly halves (73.66 cm), the dose rate will be

$$D_a = 4.63 \text{ mrad/hr or } 5 \text{ mr/hr} \quad .$$

A plot of the dose rates along the exterior core axial midline, as approximated by this method, is given in Fig. 4. The calculated results are in good agreement with experimental measurements at core-detector distances for which the Juno survey meters were considered adequate (>12 in.).

IX. TEMPERATURE CALCULATIONS

One purpose in constructing Assembly 37 was to collect information on temperature distributions and peak saturation temperatures in the core that could be used to predict temperatures that may exist in future plutonium cores.

Since ZPR-III is constructed of a large number of horizontal matrix tubes into which are inserted a variety of different materials, it was anticipated that the axial and radial conductivities may differ by an order of magnitude.

The measured axial and radial temperature distributions were fitted to parabolic functions from which thermal conductivities were calculated. These conductivities were used in conjunction with the generalized heat conduction code, GHT,[12] to calculate temperature distributions. This code solves steady-state and/or transient heat conduction problems in 3-dimensional geometry. The method used in GHT is numerical integration of the appropriate finite-difference equations. For a steady-state problem, the required input data for each nodal point is the heat generation Q and the thermal conductances K. In order to calculate the conductances from the thermal conductivities obtained from the experimental temperature distribution, the neutron-diffusion theory code CURE[13] was used. This is a generalized 2-space-dimension multigroup coding for the IBM 704, which can calculate the GHT input values for X-Y, R-Z, or R-θ geometry.

It was difficult to calculate exact conductivities from the experimental temperature distributions since the points fit parabolic functions only approximately. Therefore, some alteration of the CURE input data was required before the GHT code would calculate a temperature distribution that would approximate the experimental distribution. The results of this calculation along with a comparison of central calculated and experimental temperatures are given in Table VI. A comparison of calculated and experimental temperature distributions can be found in Figs. 17 and 18.

Table VI

CORE THERMODYNAMIC CONSTANTS AND PEAK TEMPERATURES

Radial Conductivity	(Core) $0.031 \frac{\text{Btu}}{\text{hr-in.-°C}} = 0.00154 \frac{\text{cal}}{\text{sec-cm-°C}}$
Axial Conductivity	(Core) $0.2 \frac{\text{Btu}}{\text{hr-in.-°C}} = 0.00992 \frac{\text{cal}}{\text{sec-cm-°C}}$
Radial Conductivity	(Blanket) $0.05 \frac{\text{Btu}}{\text{hr-in.-°C}} = 0.00248 \frac{\text{cal}}{\text{sec-cm-°C}}$
Axial Conductivity	(Blanket) $0.5 \frac{\text{Btu}}{\text{hr-in.-°C}} = 0.0248 \frac{\text{cal}}{\text{sec-cm-°C}}$
Calculated Peak Saturation Temperature	(42.8°C) - (109°F)
Experimental Peak Saturation Temperature	(43.6°C) - (110°F)

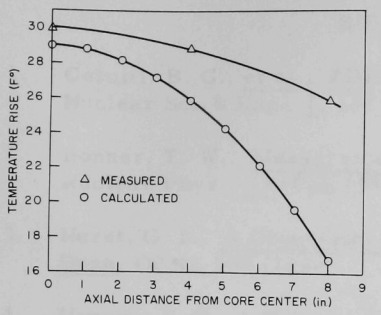

Fig. 17. Measured and Calculated Axial Temperature Rise Vs. Axial Position at Core Interface

Since matrix tube boundaries and thermal contact of pieces making up the core are probably the limiting factor in the heat flow out of the reactor, it is thought that the conductance values for future planned reactors will not deviate far from the conductivities measured for this core. Use of the conductivities given in Table VI to calculate peak saturation temperatures for future metal assemblies should prove reasonably accurate.

The temperature distributions from these calculations do not match the experimental distributions with any degree of accuracy. Although the reason for this is not completely clear, it may lie in the large difference between axial and radial conductivities.

Fig. 18

Measured and Calculated Temperature Rise Vs. Radial Position at Core Interface

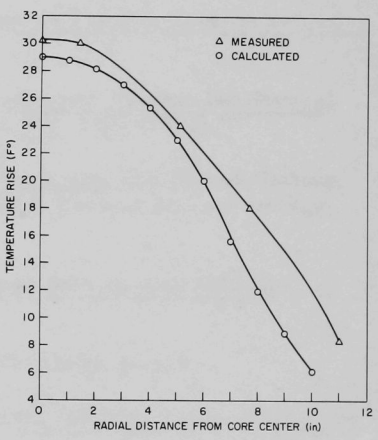

ACKNOWLEDGEMENTS

The authors are indebted to F. W. Thalgott for guidance of the experimental program of which this assembly is a part, and in particular for able assistance in setting up safe operating procedures for plutonium-fueled systems. The work of W. P. Rosenthal in editing this report and the able assistance of L. Christensen, who conducted most of the temperature measurements, are also acknowledged.

BIBLIOGRAPHY

1. Cerutti, B. C., et al., ZPR-III, Argonne's Fast Critical Facility, Nuclear Sci. & Eng., 1, 126 (1956).

2. Bonner, T. W., Measurements of Neutron Spectra from Fission, Nuclear Phys., 23 (Feb 1961).

3. Hurst, G. S., A Count-rate Method of Measuring Fast Neutron Tissue Dose, ORNL 930 (1951).

4. Hanson, A. O., A Neutron Detector Having Uniform Sensitivity from 10 kev to 3 Mev, Phys. Rev., 72, 673 (1947).

5. Loewenstein, W. B., and D. Okrent, The Physics of Fast Power Reactors; A Status Report, 2nd United Nations International Conference on the Peaceful Uses of Atomic Energy, Geneva, Switzerland 12, 16 (1958).

6. Richmond, R., Calibration of Spontaneous Fission Neutron Sources, AERE R/R 2097 (1957).

7. Crane, W., Average Number of Neutrons per Fission for Several Heavy Element Nuclides, Phys. Rev., 101, 1804 (1956).

8. Roesch, W. B., Surface Dose from Plutonium, 2nd United Nations International Conference on the Peaceful Uses of Atomic Energy, Geneva, Switzerland, 23, 339 (1958).

9. Long, J. K., et al., Fast Neutron Power Studies with ZPR-III, ibid., 12, 121 (1958).

10. Reactor Physics Constants, ANL-5800 (1958), p. 418.

11. Carlson, B. G., et al., The DSN and TDC Neutron Transport Codes, LAMS-2346 (1960).

12. Fowler, T. B., and E. R. Volk, Generalized Heat Conduction Code for the IBM-704 Computer, ORNL-2734 (1959).

13. Wachspress, E. L., CURE, A Generalized Two-space-dimension Multigroup Coding for the IBM-704, KAPL-1724 (1957).

BIBLIOGRAPHY